

# GSPMD: General and Scalable Parallelization for ML Computation Graphs

Yuanzhong Xu, HyoukJoong Lee, Dehao Chen, Blake Hechtman, Yanping Huang, Rahul Joshi, Maxim Krikun, Dmitry Lepikhin, Andy Ly, Marcello Maggioni, Ruoming Pang, Noam Shazeer, Shibo Wang, Tao Wang, Yonghui Wu, Zhifeng Chen  
Google

## Abstract

We present GSPMD, an automatic, compiler-based parallelization system for common machine learning computation graphs. It allows users to write programs in the same way as for a single device, then give hints through a few annotations on how to distribute tensors, based on which GSPMD will parallelize the computation. Its representation of partitioning is simple yet general, allowing it to express different or mixed paradigms of parallelism on a wide variety of models.

GSPMD infers the partitioning for every operator in the graph based on limited user annotations, making it convenient to scale up existing single-device programs. It solves several technical challenges for production usage, such as static shape constraints, uneven partitioning, exchange of halo data, and nested operator partitioning. These techniques allow GSPMD to achieve 50% to 62% compute utilization on 128 to 2048 Cloud TPUv3 cores for models with up to one trillion parameters.

GSPMD produces a single program for all devices, which adjusts its behavior based on a run-time partition ID, and uses collective operators for cross-device communication. This property allows the system itself to be scalable: the compilation time stays constant with increasing number of devices.

## 1 Introduction

Recent development of neural networks has shown dramatic benefit from model scaling, creating a demand to parallelize computation in terms of both training data and model parameters. Parallelism may be introduced in several ways: data parallelism [19] partitions training data, pipeline parallelism [15, 22, 24] partitions the computation graph, and within-layer model parallelism [35] partitions the weight and computation of each model layer.

We present GSPMD<sup>1</sup>, a system that uses simple *tensor sharding annotations* to achieve different parallelism paradigms in a unified way, including data parallelism, in-layer model parallelism, and novel strategies like image spatial partitioning [11] and weight-update/optimizer-state sharding [28, 38]. Although pipeline parallelism partitions the graph instead of individual operators/tensors, GSPMD could still achieve it

with the help of a simple wrapper library that reduces pipelining to a tensor/operator partitioning problem. GSPMD is flexible enough to express combinations of these approaches, e.g., different layers could be partitioned in different manners, and different approaches could be combined in the same layer.

GSPMD separates the concerns of machine learning model programming and parallelism. It allows users to write programs with giant tensors as if there were a single giant device. Then the user can insert annotations in a few key places in the model that specify how tensors are distributed across devices; GSPMD will run compiler passes that complete the sharding specification on the entire computation graph, and transform it into a semantically equivalent, parallelized computation to run on each device. This property allows the users to focus on model building instead of sharding implementation. It also enables easy porting of legacy single-device programs to run at a much larger scale. When experimenting with different partitioning strategies, the user needs to reconfigure only the annotations.

GSPMD addresses several practical issues when applying automatic partitioning to production models:

- Generating one program for each partition would increase compilation time significantly when there are many partitions, so GSPMD instead produces a single program for all partitions. The behavior of the produced program is controlled by a run-time partition ID. This is a property we call Single Program Multiple Data (SPMD), and is crucial for scaling the system to thousands of partitions.
- GSPMD supports unevenly partitioned dimensions, which allows any tensor to be partitioned on an arbitrary mesh of devices.
- We implemented GSPMD as an extension to a production ML compiler, XLA [2]. The implementation covers the full set of operators in XLA, including those with complicated semantics. For example, `Convolution` has a flexible configuration space including padding and dilation [1]. XLA can be used as a unifying abstraction for multiple front-end frameworks (TensorFlow [5], Jax [7], Pytorch [27] and Julia [6]) and multiple hardware platforms (CPUs, GPUs and Cloud TPUs [14]), making GSPMD's core implementation reusable.
- GSPMD does not require the accelerator platform to support dynamic tensor shapes or operator configurations. It is often a practical constraint for accelerators to require

<sup>1</sup>GSPMD is generalized from the back-end system used in our earlier work GShard [20].

statically known shapes at compile time, in order to ease high-performance operator development. This constraint makes it challenging to partition certain cases where partitions have different conceptual shapes or configurations. We solved this problem by generating equivalent static operators using padding and slicing with dynamically computed offsets.

- GSPMD supports nested patterns of parallelism; at per-operator level, that means different types of dimensions could be partitioned across orthogonal subgroups of devices. We have developed a recursive method for such nested patterns, maximizing the generality of GSPMD without requiring excessive handwritten partitioning rules.

We demonstrate the capability of GSPMD by applying it on several categories of ML model, and measuring the performance and memory scaling of model training on thousands of Cloud TPUv3 [14] devices. The use cases include image models, and sparse and dense language models. By choosing intuitive initial annotations, we can achieve close-to-linear memory and performance scaling with respect to the number of devices.

## 2 Background

Modern ML models are typically defined as dataflow graphs of connected layers (subgraphs). Each layer has its model weights/parameters, and produces outputs that are referred to as “activations”. Model training requires first computing the model’s final output (forward pass), then computing the gradients of each layer weight (backward pass), which happens in the reverse layer order due to backward data dependencies. Model serving requires only the forward pass.

### 2.1 Common parallelism patterns in ML workloads

Below are a few typical parallelism patterns used in modern ML workloads.

**Data parallelism** is a technique for parallelizing training [19]. Different devices (replicas) have the same copy of the model, but compute on different training data to produce local gradients. They collect and sum their gradients to keep in sync with each other. Such synchronization is typically implemented as an MPI-style AllReduce operator [23].

**Within-layer model parallelism** partitions the weight tensor of a layer across multiple devices [35]. It may also require communication across devices, e.g., AllReduce when the layer sums over a partitioned dimension. Compared to data parallelism, this technique can help building larger models by sharding the weights.

**Spatial partitioning** is a technique to shard image input data along spatial dimensions [11], which helps fitting large image data on devices with limited memory capacity.

**Weight-update sharding or optimizer-state sharding** is an enhancement to data parallelism where the computation to apply combined gradients onto weights is sharded across

replica devices [28, 38]. It is a performance and memory optimization especially for expensive optimizers like ADAM [18].

**Pipeline parallelism** partitions the training graph into multiple stages that run on different devices [15] to help build large models. Each stage sends its result to its downstream stage in the forward pass, and to its upstream stage in the backward pass. Due to data dependencies between the forward and backward passes, devices can be idle during part of the training step, which is known as a “bubble”. The overhead of bubbles can be amortized with larger global training batch size. Pipelining can also help build large models.

GSPMD is designed to be a general solution for all of the above types of parallelism. It natively supports **in-operator** parallelism, which includes everything above except pipelining. Although pipeline parallelism is not in-operator partitioning, it could be **reduced to an operator partitioning** problem with the help of a wrapper library over legacy code (Section 3.3) in some common cases, and GSPMD could still be used to shard individual stages in combination with existing pipelining implementation for unsupported cases.

More importantly, GSPMD can easily express **nested patterns** of the above techniques. Section 5 shows examples of combining them in the Transformer [37] model.

### 2.2 XLA and TensorFlow

The automatic partitioner in GSPMD is implemented as transformation passes in the XLA compiler [2]. XLA defines a backend-agnostic intermediate representation (IR) called HLO, which models a computation as a dataflow graph where nodes are operators and edges are tensors. There are simple elementwise arithmetic operators like Add and Multiply, a general matrix multiply operator Dot, windowed operators like Convolution, and data-formatting operators like Reshape and Transpose.

Multiple front-end frameworks including TensorFlow [5], JAX [7], PyTorch [27] and Julia [6] already have lowering logic to transform their graph representation to XLA HLO graph, which can then be compiled into target executables if the accelerator has a compiler backend for XLA. XLA has a much smaller set of operators than front-end frameworks like TensorFlow. This reduces the burden of implementing a partitioner without harming generality, because the existing lowering from frontends performs the heavy-lifting to make it expressive. Although we developed the infrastructure in XLA, the techniques we describe here can be applied to intermediate representations in other machine learning frameworks (e.g., ONNX [3], TVM Relay [29], Glow IR [30]).

In this paper we demonstrate the use cases with models written in TensorFlow. TensorFlow offers a Python API for defining and running ML models. A component called the *TF2XLA bridge* transforms the TensorFlow model into an equivalent XLA graph, so that XLA can compile it into a device executable.

### 3 Tensor Sharding and Auto Completion

GSPMD defines an intuitive and general representation of tensor sharding. Following the philosophy of separation of concern, GSPMD has two independent compiler transformations: sharding completion and per-operator partitioning.

#### 3.1 Representation of tensor sharding

In GSPMD, each tensor will be assigned a **sharding** property, either explicitly by the user as initial annotations, or by the sharding completion pass. The sharding property specifies how the data is distributed across devices. GSPMD defines three types of sharding (see also Figure 1).

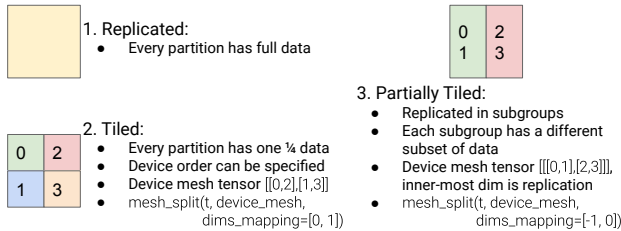


Figure 1. Examples of the three types of sharding on a data tensor, and the `mesh_split` API calls to represent them.

- Replicated. All devices have the same full data.
- Tiled. A tiled sharding contains a multi-dimensional tensor consisting of device IDs (e.g.,  $[[0,2],[1,3]]$  in Figure 1), which must have the same rank as the data tensor. Each data dimension is sharded across devices along the same dimension in the device tensor, and each device occupies the corresponding tile in the data tensor that matches its location in the device tensor. There is zero data duplication.
- Partially tiled. The devices are first divided into equally sized subgroups, and the data tensor is replicated across devices in each subgroup but tiled across subgroups. Internally, it is also represented as a tensor of device IDs, with an additional dimension at the end for replication subgroups.

This representation is simple yet general, because it treats all tensor dimensions in the same way and does not specialize for batch dimensions (data parallelism [19]), weight dimensions (model-parallelism or weight-update sharding [38]), or image dimensions (spatial partitioning [11]).

GSPMD provides a convenient abstraction on top of the above low-level sharding representation. Devices can be organized in a logical multi-dimensional tensor called a **device mesh**, which can be used with an intuitive API.

`mesh_split(tensor, device_mesh, dims_mapping)` is the primary API GSPMD provides for users. It generates a sharding annotation for tensor, based on the device mesh and a mapping from each data tensor dimension (i) to an optional device mesh dimension (`dims_mapping[i]`). It uses -1 to represent a non-existing mapping in `dims_mapping`. Each device mesh dimension should appear at most once in

`dims_mapping`. This simple API is general enough to express all three types of sharding.

- When `dims_mapping` is all -1's, no dimension is sharded in the data tensor, so it will create a replicated sharding annotation.
- When `dims_mapping` contains all of the mesh dimensions, the data tensor is fully sharded across all devices, so it will create a tiled sharding annotation.
- When `dims_mapping` contains part of the mesh dimensions, the data tensor is partially sharded, so it will create a partially tiled sharding annotation.

When generating collective communication operators, GSPMD preserves the order of devices in `device_mesh`. Therefore, `device_mesh` can be configured by the user in order to optimize communication based on the topology of the device network. For example, it could model the actual topology of device network, or reorder devices to avoid long links.

In typical use cases, the user only needs to define the device mesh once, and then focus on the mapping of tensor dimensions. However, GSPMD does not have any restrictions if the user wants to use a different device mesh for each tensor. This could be useful when different parts of the model have very different parallelism patterns.

#### 3.2 Examples of expressing in-operator parallelism

To help the discussion, we first explain a useful and succinct operator in TensorFlow (and other libraries like numpy), the *Einstein Summation* or Einsum. The equivalent operator in XLA is Dot. It is a generalized matrix multiply, where the user can define arbitrary numbers of dimensions of different types. An Einsum can be expressed as a string equation, e.g.,  $ABC, ACD \rightarrow ABD$ , where  $A$  is an embarrassingly parallel *batch* dimension in both operands and the output,  $C$  is a *contracting* dimension that only exist in the operands and will be sum-reduced, while  $B$  and  $D$  are *non-contracting* dimensions that exist in one operand and are inherited by the output.

With GSPMD, the user can annotate the operands and the output to combine different parallelism modes. For a typical fully connected projection layer,  $BD, DF \rightarrow BF$ , the user can combine data- and model-parallelism by annotating

```
bd = mesh_split(bd, mesh, [0, -1])
df = mesh_split(df, mesh, [-1, 1])
```

and GSPMD will auto-complete the output sharding with `mesh_split(bf, mesh, [0, 1])` so that the input and output are partitioned on the batch dimension (data-parallelism) across mesh dimension 0, while the layer weight `df` and the output are partitioned on the feature dimension F (model-parallelism) on mesh dimension 1.

If the user further partitions the weights along the other mesh dimension, i.e.,

```
df = mesh_split(df, mesh, [0, 1])
```

it will additionally trigger the weight-update sharding optimization [28, 38] where the weight will be unsharded on

demand on the D dimension right before this layer in the forward pass to reduce peak memory usage, and gradients will be communicated with ReduceScatter instead of AllReduce in the backward pass and applied on a sharded optimizer.

If the layer has a sparsely activated mixture-of-expert (MoE) architecture [33], it can additionally have an expert E dimension in the Einsum equation on both operands and the output, i.e.,  $EBD, EDF \rightarrow EBF$ . To parallelize the experts across different devices, the user only needs to annotate the E dimension on these tensors, e.g.,

```
ebd = mesh_split(ebd, mesh, [0, -1, -1])
edf = mesh_split(edf, mesh, [0, -1, 1])
ebf = mesh_split(ebf, mesh, [0, -1, 1])
```

In practice, the annotations on the activations ebd and ebf can be omitted and GSPMD can infer them from the weights, unless the upstream or downstream layers have a different pattern of parallelism.

### 3.3 Pipeline parallelism reduced to tensor sharding

Pipelining does not partition individual operators or tensors, but partitions the graph into *pipeline stages*. We consider a constrained scenario of pipelining: all stages are the same subcomputation except for having different weight values. This constraint is practical because a common way to scale up models is to stack layers of the same pattern [8, 15].

We reduce pipelining into a layer-wise sharding problem. Imagine that the layer computation is rewritten in a stage-parallel way, where a leading layer/stage dimension L has been added to each tensor, and the computation is entirely parallel on this dimension. This transformation can be done by existing frontends' vectorization support like JAX's vmap() and TensorFlow's vectorized\_map().

Pipelining requires data to be organized into *microbatches*; each stage loops over them one at a time [15]. We use a *shifting buffer* to pass data across stages, and it also has a leading L dimension, as shown below.

```
# Shifting buffer.
state = zeros([L, ...])
for i in range(num_microbatches + L - 1):
    # Shift state to the right by 1.
    from_prev_stage = pad_right(state, 1)[1:]
    stage_ids = range(L) # [0, 1, 2, ...]
    inp = next_input()
    input = elementwise_select(
        stage_ids == 0, inp, from_prev_stage)
    state = vmap(OneStageCompute)(input, ...)
```

The above is the Python code for the forward pass of vectorized pipelining. During each iteration, the state buffer is shifted to the right by one along L, so that the previous layer's last result is passed to the next layer. The loop runs additional stages - 1 iterations to wait for the last stage to finish processing all the microbatches. The extra iterations are equivalent to the *bubbles* in earlier work [15] that describe the

idle time due to data dependency, although here the waiting devices compute on padded data instead of being idle.

With the help of vmap or vectorized\_map, this loop implementation can wrap a legacy single-stage implementation OneStageCompute and turn it to a pipelined computation.

This user-level loop library does not implement distributed execution, and it runs on a single device. To distribute it on multiple devices, users can simply annotate the L dimension to be sharded, and GSPMD will turn the buffer shifting into cross-device communication via CollectivePermute.

There are several benefits of this pipelining implementation. First, it runs naturally when combined with other types of parallelism in GSPMD, avoiding the need for extra infrastructure. Second, it benefits from the SPMD property, so that the infrastructure is very simple and does not need to maintain the interface between multiple programs. However, it is limited to homogeneous pipeline stages; for heterogeneous stages we recommend integrating GSPMD with other pipeline implementations [15, 22, 24] and sharding each stage.

### 3.4 Intuitive sharding completion

This section describes how GSPMD auto-completes the sharding on every tensor based on limited user annotations. It is implemented as a compiler pass in XLA. A design goal is to make the sharding decisions **intuitive** to users even if they only annotate a small subset of tensors.

**Preserved dimensions in operators.** GSPMD could infer the sharding on every tensor based on limited user annotations, because XLA operators typically preserve some dimensions from inputs to outputs. We simply propagate sharding of such a dimension from inputs to outputs, and vice versa. For example, a sharding annotation on the input batch dimension could be propagated down to all layers' results (activations), and the same is true for image spatial dimensions.

We decided to keep the sharding propagation simple, so it does not try to create new sharding patterns on dimensions. The propagation result may not always be optimal, but results will be the most intuitive to users. Users may insert more sharding annotations to instruct GSPMD to partition each tensor as desired.

In comparison, a fully automatic approach could apply advanced algorithms to find the best partitioning strategy (e.g., [16] on model inference) beyond user annotations, but it is still an open problem for large-scale training tasks. GSPMD instead focuses on propagating user intentions, though it may also be useful in defining the search space for a fully automatic approach.

**Merging compatible shardings.** The result of an XLA operator can inherit dimensions from different inputs. For example, the Dot operator is a generalized matrix multiply, and GSPMD infers sharding based on each operand; when the inferred shardings from the operands are different, GSPMD combines them if they are compatible to form a more refined

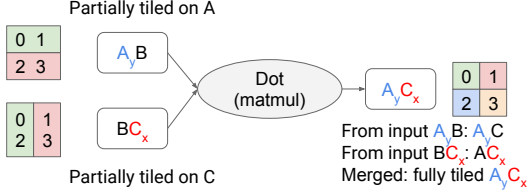


**Figure 2.** Sharding propagation through a Dot operator. The result is merged from both inputs. Different colors and subscripts of the letters represent sharding along different device mesh dimensions.

sharding. A typical example of compatible shardings is two orthogonal partially tiled shardings created by `mesh_split` on different tensor dimensions, as shown in Figure 2.

More formally, we use  $Offset(S, d, i)$  to denote the *shard offset* of device  $d$  in dimension  $i$  according to sharding  $S$ . The shard offset describes the location of the device’s data partition within the original shape before partitioning. Then, two shardings  $S_0$  and  $S_1$  are compatible with each other if there exists a sharding  $S$  where for each device  $d$ ,

$$Offset(S, d, i) == Offset(S_0, d, i)$$

for every sharded dimension  $i$  in  $S_0$ , and

$$Offset(S, d, j) == Offset(S_1, d, j)$$

for every sharded dimension  $j$  in  $S_1$ . In this case,  $S$  is a merged sharding of  $S_0$  and  $S_1$ .

Merging compatible shardings is the key to support nested parallelism patterns with simple user annotations. For example, if the user wants to mix data- and model-parallelism, they could simply annotate the inputs to be sharded on the batch dimension along one device mesh dimension, while the layer weights are sharded on certain model dimensions along other mesh dimensions. This way, the result of this layer will be propagated with sharding on both dimensions.

**Iterative, priority-based sharding propagation.** To complete the sharding assignment on all tensors, GSPMD runs the propagation pass on the entire graph in multiple iterations, and alternates between forward propagation (input to output) and backward propagation (output to input). While it preserves initial user annotations, shardings assigned by the pass could be refined incrementally over the iterations. This means it changes the sharding on a tensor only when it finds a more fine-grained sharding (possibly by combining with existing compatible sharding). This property guarantees the pass could reach a fixed point after finite iterations.

In practice, some use cases would require switching the sharding on a dimension in different tensors, as shown in Section 5. In this case, the sharding decision on each tensor will depend on the order in which the propagation pass iterates over the operators. To produce the most intuitive sharding assignment, GSPMD assigns a priority to the propagation through each operator from each direction.

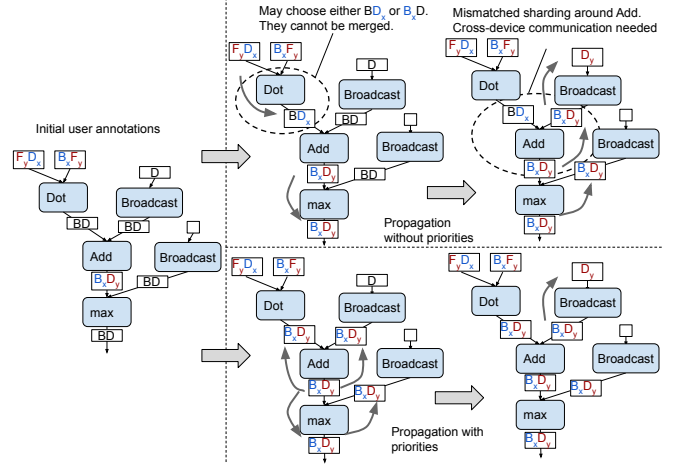


**Figure 3.** Comparison between sharding propagation algorithms with and without priorities. The top-right figure shows a potential propagation process without priority, where tensors are visited in a topological order; since there are multiple ways to propagate through Dot, it may result in mismatched sharding specifications around an elementwise operator. The bottom-right figure shows the propagation process when elementwise operators are given a higher priority, where all the BD-shaped tensors are assigned the same sharding specification.

GSPMD assigns the elementwise operators the highest priority to propagate through in both directions, because all inputs and outputs have the same shape and there is no cross-element computation. Propagating through elementwise operators would be the most intuitive decision from the user’s point of view. Operators like Dot, which adds or removes dimensions are assigned lower priority. We also assign different priorities to different directions; for example, the Broadcast operator adds dimensions to the input by duplicating the data, so we assign higher priority to the backward propagation, which helps to avoid potential communication on the larger shape due to mismatched shardings. See Figure 3 for the sharding propagation processes with and without priorities on a typical linear layer followed by a ReLU activation function.

**Guide for users.** Sharding propagation allows the users of GSPMD to skip manual annotations on many intermediate results, such as those produced by layers like ReLU and Batch Normalization. If users want explicit control over sharding decisions, especially when tensors are sharded differently along a logical dimension, they could focus on operators that significantly change the dimensions. For example, if the inputs of a dot operator do not have compatible shardings, there are multiple ways for the sharding propagation to infer the output sharding; the user can explicitly annotate the output to precisely control the sharding decision.

### 3.5 API Integration in high-level frameworks

GSPMD’s sharding API is essentially an annotation on unpartitioned graphs. We created a wrapper operator in TensorFlow, `XlaSharding`, to allow users to instrument GSPMD by writing regular TensorFlow programs. From the user’s point of view, `XlaSharding` is semantically equivalent to an `Identity` operator that passes the input through unchanged, but the sharding annotation can be specified as an attribute. The TF2XLA bridge preserves the annotation when converting the TensorFlow program to an XLA program. Other than specifying the initial sharding annotations, the user could largely reuse legacy unpartitioned TensorFlow programs. Users can also conveniently reconfigure the program to different device cluster topologies by changing the sharding annotations and keeping the rest of the program unchanged.

Frameworks like TensorFlow also support automatic gradient calculation, where they generate the backward computation and gradients of each model weight based on the user’s model definition (forward computation). It is done by composing the gradient computation of operators in the graph, which requires each operator to have a registered gradient computation. We define the gradient of `XlaSharding` to be a copy of itself. In this way, the backward computation will be annotated automatically with the same sharding.

## 4 The SPMD Partitioner

Once every tensor in the graph is assigned a sharding, the remaining work for GSPMD is to rewrite each operator to an equivalent partitioned computation which potentially includes cross-partition communications.

There are two options when implementing the partitioner: 1) creating a customized program for each of the partitions (Multiple Programs Multiple Data, or MPMD), and 2) creating a single program that works for all partitions (Single Program Multiple Data). We choose SPMD because we aim to scale up to thousands of partitions, where compiling the many programs would be prohibitively slow in MPMD. Compilation time is an important usability concern because modern ML frameworks often include JIT optimizations and compilation, especially for those targeting custom accelerators [2, 9, 30], and parallelizing the compilation can be non-trivial because operators in different programs may need to be globally scheduled to maintain correct communication order.

However, implementing the partitioner in SPMD creates unique challenges for production ML compilers. This section covers the challenges for SPMD partitioning and the techniques we use to solve them.

### 4.1 Static constraints

**Static shapes.** ML accelerators get their performance edge via specialized hardware, such as vector and matrix units. In practice, the XLA compiler supports only limited degree of

dynamism in tensor shapes, in order to ease the development of highly efficient operator kernels.

GSPMD is designed to work even with full static shape constraints, but static shapes create a challenge for SPMD partitioning. When a computation is partitioned, it’s not always the case that all partitions have the same input/output shapes, because dimensions may not be evenly divisible by the number of partitions. In those cases, GSPMD rounds up the size of the shape to a multiple of partition count, and the data in that padded region can be arbitrary.

When creating certain partitioned operators, data in the padding area needs to be masked off. For example, a `reduce` operator needs to prevent the padding data from affecting the result, so GSPMD first replaces them with the identity value of the reduction.

The amount of padding can vary between different partitions. Although shapes are static, several XLA operators accept dynamic offsets as operands, which allows GSPMD to express dynamic padding area as a function of the partition ID. Table 8 in the Appendix summarizes the important XLA operators that GSPMD relies on for dynamism and masking. For example, masking padded data can be expressed as a `Select` according to a mask calculated by comparing `Iota` and an offset based on `PartitionId`.

**Static operator configurations.** XLA operators also have static configurations, like the padding, stride, and dilation defined in `Convolution`. However, different partitions may not execute with the same operator configuration. E.g., for a `Convolution`, the left-most partition applies padding to its left while the right-most partition applies padding to its right. In such cases, the partitioner chooses a conservative configuration that makes some partitions to produce slightly more data than needed, then slices out the the irrelevant parts.

### 4.2 Communication primitives

Since the partitioner forces all the devices to run the same program, the communication patterns are regular. We use XLA’s operators that provide MPI-style collective communications [23]. **CollectivePermute** exchanges data among a list of source-destination pairs. **AllGather** concatenates tensors from all participants following a specified order. **AllReduce** performs elementwise reduction (e.g., summation) over the inputs from all participants. **AllToAll** logically splits the input of each participant along one dimension, then sends each piece to a different participant. On receiving data pieces from others, each participant concatenates the pieces to produce its result. **ReduceScatter** is semantically equivalent to an `AllReduce` followed by a `DynamicSlice` where each partition gets one slice of the fully reduced data. An efficient implementation has only half the cost of `AllReduce`.

### 4.3 Halo exchange with dynamic bounds

Certain operators have a communication pattern which involves partial data exchange with neighboring partitions, which we call *halo exchange*. We use the `CollectivePermute` operator to exchange halo data between partitions.

**Windowed operators.** The most typical use case of halo exchange is for partitioning window-based operators (e.g., `Convolution`, `ReduceWindow`), because neighboring partitions may require overlapping input data (Figure 4a). In practice, halo-exchange for these operators often needs to be coupled with proper padding, slicing, and masking due to advanced use of window configurations (dilation, stride, and padding), as well as uneven halo sizes.

**Non-constant halo size.** The amount of halo data needed by different partitions are often different. In such cases, GSPMD uses maximum halo size across partitions, then uses `DynamicSlice` to remove excessive data in the halos. See Appendix A.2 for a concrete example. GSPMD supports the full set of configurations in the XLA `Convolution` operator, including arbitrary padding and dilation. These configurations add further complexity to the partitioner, but this can be ameliorated by applying careful padding and slicing.

**Halo exchange for data formatting.** Another use of halo exchange is for data formatting operators that change the size of the shape. For example, after a `Slice` or `Pad` operator, the shape of the tensor changes, and so do the boundaries between partitions. This requires us to realign the data on different partitions, which can be handled as a form of halo exchange (Figure 4b).

Other data formatting operators may need halo exchange even when not changing the size, because the partitions may be uneven and the shapes are constrained to be static. For example, the `Reverse` operator reverses the order of elements in a tensor, but if it is partitioned unevenly, we need to shift data across partitions to keep the padding logically to the right of the result tensor. Another example is `Reshape`. Consider reshaping a tensor from (3, 2) to (6), where the input is unevenly partitioned in 2 ways on the first dimension (partition shape (2, 2)), and the output is also partitioned in 2 ways (partition shape (3)). There is padding on the input due to uneven partitioning, but after `Reshape`, the output tensor no longer has padding; as a result, halo exchange is required in a similar way to `Slice` (Figure 4c).

### 4.4 Grouping and recursive partitioning

Many XLA and TensorFlow operators are rank polymorphic, where the same opcode can be used on tensors with arbitrary number of dimensions; a classic example is the `Einsum` operator as we discussed in Section 3.2. GSPMD’s generic annotation API makes it convenient to combine different parallelism modes by sharding multiple dimensions, so there is a need for the partitioner to recognize not only fixed patterns

but also nested cases. In order to avoid manually writing partitioning rules on all combinations of patterns, we developed a framework (Figure 5) to recursively pattern-match each set of sharded dimensions, and partition nested cases.

First, we introduce a device context object for the partitioner, which defines how cross-partition collective operators are created based on given subgroups of devices, and how the partition ID is calculated. This context generalizes the concept of devices as virtualized *logical partitions* via custom factory methods of collective operators and partition IDs.

Second, we introduce partition grouping. We can divide the devices into equally sized groups, and treat each group as a logical partition. Once we have such grouping, we can create a new partitioner context, where each logical partition is mapped to a group of devices. Within this context, whenever a collective operator is created, the logical IDs of the participants are rewritten to subgroups of original device IDs.

With this approach, GSPMD can perform recursive pattern matching on an `Einsum` op. For example, the partitioner detects whether there is a matching pattern on how the batch dimensions are partitioned in the inputs and the output. If such a batch-partitioned pattern exists, it could create a nested partitioner context by grouping the partitions across the batch dimensions and reducing the shape sizes; then it recursively calls the partitioner to handle other dimensions. Recursive partitioning allows us to handle nested partitioning cases without having to enumerate all possible combinations.

This technique greatly simplifies the partitioner’s implementation of operators with rank polymorphism and complicated dimension configurations. For example, we applied it to `Convolution`, which allows the user to combine spatial partitioning and feature partitioning in the same operator.

### 4.5 Resharding

GSPMD always produces a valid partitioned graph regardless of what sharding annotations are provided. If the provided shardings are not the typical supported cases, the partitioner will perform *resharding* on the inputs and/or outputs. The resharding operation may involve cross-device communications, and we list the different types of resharding below.

- To replicate data along sharded dimensions, the partitioner uses `AllGather`. The `AllGather` in Figure 5 is an example of this type of resharding.
- To switch the sharding along one tensor dimension to another tensor dimension, the partitioner uses `AllToAll`.
- To change the order of devices, the partitioner uses `CollectivePermute`.
- To shard a replicated dimension, the partitioner uses `DynamicSlice`. There is no communication in this case.

The partitioner could use multiple steps of resharding to reach the desired sharding. In the worst case, when none of the above cases could be applied, the partitioner will first fully replicate the tensor, then shard it in the desired way.

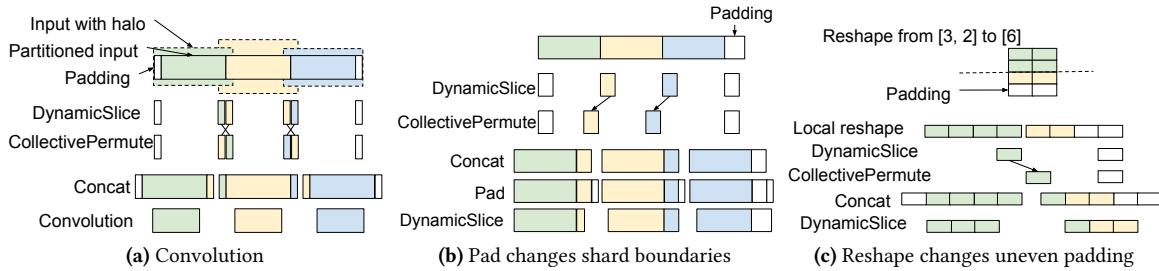


Figure 4. Halo exchange examples. Different colors represent data from different partitions.

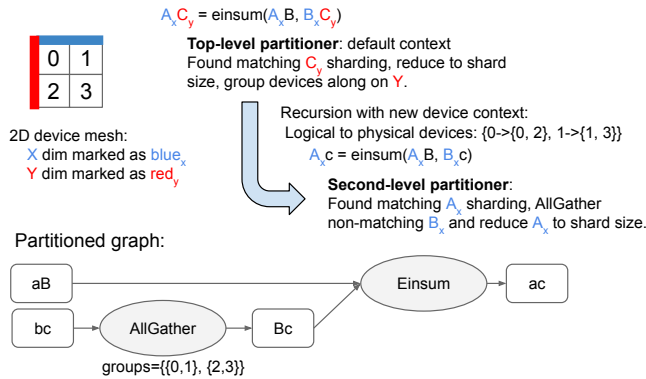


Figure 5. Recursive partitioning of  $AC = \text{einsum}(AB, BC)$ . Letters in blue indicate dimensions sharded on the X dimension of the device mesh, while letters in red indicate dimensions sharded on the Y dimension. Lower case letters indicate sharded size. AllGather is created by the inner partitioner, where logical subgroups  $\{0,1\}$  are rewritten to  $\{\{0,1\}, \{2,3\}\}$  according to the context.

#### 4.6 Compiler optimizations for data formatting

**Pre-processing.** Certain transformations may help produce faster programs simply by rearranging the data. For example, a data rotation pattern  $\text{Concat}(a[k:], a[:k])$  that moves the first  $k$  elements to the end can be recognized to avoid multiple rounds of halo exchanges in  $\text{Slice}$  and  $\text{Concat}$ . XLA does not define such an operator, but we define a custom  $\text{SPMD\_Rotate}$  within the partitioner. Similar optimizations include merging a sequence of  $\text{Pad}$  and  $\text{Slice}$  operators, which is important to partition the pipelined program in Section 3.3 where the shifting using  $\text{Pad}$  and  $\text{Slice}$  can be done with a single  $\text{CollectivePermute}$ .

**Post-partitioning optimizations.** The partitioner creates various data formatting operators in order to perform slicing, padding, concatenation, masking and halo exchange. We leverage XLA’s fusion capabilities, as well as new code motion optimizations for slicing and padding, to largely hide the overhead of data formatting. As a result, the run-time overhead is typically small.

## 5 Case Study and Evaluation

This section demonstrates a few cases where we apply GSPMD to widely-used language and image models to scale up either the model size and the input size.

We measure the model performance with GSPMD on the Cloud TPUv3 platform [14], which has an XLA compiler backend so that it can execute the partitioned graphs produced by GSPMD. Each TPUv3 core has 16GB on-device memory, and the platform has high-speed homogeneous device-to-device links across many cores even if they are hosted on different machines, and these links form a 2D mesh. Such a platform is ideal to study the scalability of GSPMD, which achieves high compute utilization with operator sharding alone. Nonetheless, we also study pipeline parallelism combined with operator sharding in Section 5.2, which could be more practical for GPU platforms<sup>2</sup> where high-speed links only exist within a server host.

### 5.1 Dense Transformer language model

Transformer [37] is a widely-deployed model for tasks including translation, text generation and understanding. Its core consists of two alternating types of layers. Suppose the input to such layers is a tensor of shape  $(B, S, M)$ , where  $B$  is the sample batch size,  $S$  is the sequence length per batch, and  $M$  is the model dimension for features.

The *attention* layer can be described as:

$$y = \text{Attention}(W_Q \times x, W_K \times x, W_V \times x) \times W_O$$

where each of  $W_Q, W_K, W_V$  is a weight matrix that projects  $x$  into a tensor of shape  $(B, S, N, D)$ . The  $N$  dimension is called the “attention heads”, a parallel dimension during the computation of  $\text{Attention}()$ . The  $W_O$  weight matrix projects the attention result back to shape  $(B, S, M)$ .

The *feed-forward* layer can be described as

$$y = \text{Relu}(W_{in} \times x) \times W_{out}$$

where  $W_{in}$  is a weight matrix that projects  $x$  into a tensor of shape  $(B, S, H)$ ,  $\text{Relu}()$  is elementwise, and the  $W_{out}$  weight matrix projects the result back to shape  $(B, S, M)$ . In the rest

<sup>2</sup>We have enabled GSPMD in XLA’s GPU backend and verified its correctness, but do not have large-scale measurements at the moment.

of the section, we refer to the combination of one attention layer and one feed-forward layers as one *Transformer layer*.

Recent research has shown the benefit of scaling up the Transformer model [8, 15, 32] by increasing the number of layers and the sizes of dimensions M, H and N, which could reach hundreds of billions of parameters. We show that GSPMD allows these models to be trained efficiently by annotating just 7 tensors per Transformer layer (roughly 0.7% of all tensors in the entire XLA graph). Internal attention computation and other layers like normalization do not need annotations, since GSPMD can find reasonable shardings automatically.

**2D sharding.** One main goal of sharding is to make sure the model weights could fit into accelerator device memory. We study a 2-dimensional sharding strategy that aims to scale to very large model sizes. We define the device mesh as a matrix of shape (X, Y), and annotate the tensors as specified in Table 1. We choose 2D mesh for 2 reasons: 1) it maps to the 2D topology of the TPU platform’s device network, and 2) sharding a single dimension to a very small size would affect the compute efficiency on TPUs. We study 3 types of sharding configurations.

In a vanilla approach (2D Attempt 1 in Table 1), we shard H and N along Y, and M along X. The sharding annotations are consistent on all weight and activation tensors, which avoids any resharding cost. After each matrix multiply on sharded weights, GSPMD will add a subgrouped AllReduce to combine partial results. However, there are two problems: 1) the activations are only partially sharded along either X or Y, so that activation storage between forward and backward passes during training becomes the bottleneck for scalability; 2) the per-device weight is so small that it affects compute efficiency on TPUs.

Another approach (2D Attempt 2 in Table 1) is to use the same weight shardings, but switch the activations’ X sharding to the batch dimension. Weights and activations have mismatching sharding along X, so GSPMD will perform subgrouped AllGather to unshard weights along X before each layer, but this avoids the need for AllReduce on BSH. This AllGather will not increase peak memory usage significantly since it is short-lived and the buffer will be freed as soon as the layer completes. In the backward pass, GSPMD will add a ReduceScatter on gradients due to batch and weight sharding on X. This behavior along X is conceptually the same as the weight-update/optimizer-state sharding technique [28, 38]. This approach solves the compute efficiency problem, but it still suffers from an activation memory problem since the BSM tensor is still partially sharded.

In our finalized sharding configurations (2D finalized in Table 1), we enhance Attempt 2 by further sharding the BSM activation’s M dimension along Y. GSPMD will add a subgrouped AllGather for BSM to unshard M at the beginning of each layer, and replace the AllReduce on the output BSM with a ReduceScatter. The two new collective operators combined

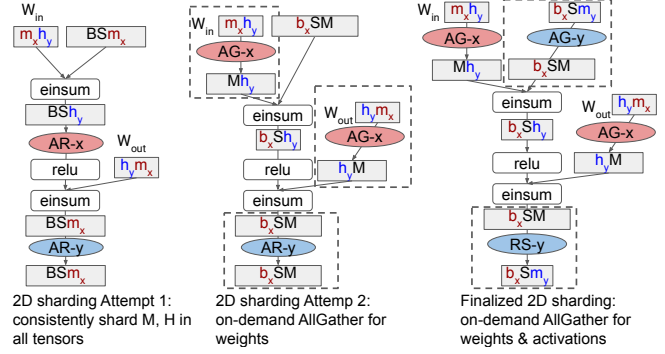


**Figure 6.** Partitioned graphs for a Transformer feed-forward layer produced by GSPMD with the sharding annotations in Table 1. Lower-case letters indicate sharded dimensions, where different colors and subscripts denote different mesh dimensions. Collective operators: AR is AllReduce, AG is AllGather, and RS is ReduceScatter.

have comparable performance to the original AllReduce. In this approach, all long-lived tensors are fully sharded across all devices, so that peak memory can scale linearly when we increase the number of devices. We are now also able to use a relatively large batch size, which further helps TPU compute efficiency. This sharding configuration combines the benefit of data parallelism, weight-update sharding [28, 38] and in-layer model parallelism [35], and only requires 7 annotations in the model. Figure 6 shows the partitioned graphs for the 3 approaches.

**Performance experiments.** To evaluate the scalability of GSPMD, we measure the performance of training Transformer models that have many layers of large weights. We choose the following dimension sizes: M is 8192, H is 65536, N is 128, D is 256, and the vocabulary size is 32000. These dimensions are comparable to GPT-3 [8]. We use a sequence length of 1024 for each input sample. Each Transformer layer (attention + feed-forward) has 2 billion parameters. We use 32-bit floating-point parameters, 16-bit floating-point activations, and Adafactor optimizer [34].

Scalability is evaluated by 2 sets of experiments: 1) a fixed model size (32 layers, 64B parameters) on different device topologies, and 2) different model sizes (32, 64, 128 and 256 layers) on a fixed device topology. Making the model deeper is more difficult than making it wider, because both compute and memory scale linearly with the model depth; in contrast, if we increase per-layer size to 4x by doubling the size of M, H and N, the activation memory only increases by 2x.

Table 2 shows the training performance of the above model configurations on the TPUv3 platform. GSPMD achieves close to linear scaling for such models, in terms of both memory and performance. For the 32-layer model, when we increase the number of TPU devices by 2x, we can roughly double the maximum input batch size, while maintaining similar step time (within 10%). On the same 2048-core device mesh, when

Shardings		$W_Q, W_K, W_V$	$W_O$	$W_{in}$	$W_{out}$	Activations			Memory usage	Communication
	Shape	MND	NDM	MH	HM	BSM	BSND	BSH	weight + activation	weight + activation
	2D Attempt 1	X,Y,-	Y,-,X	X,Y	Y,X	-,-,X	-,-,Y,-	-,-,Y	$O(1/(XY)) + (O(1/Y)+O(1/X))$	$0 + (O(1/Y)+O(1/X))$
	2D Attempt 2	X,Y,-	Y,-,X	X,Y	Y,X	X,-,-	X,-,Y,-	X,-,Y	$O(1/(XY)) + O(1/X)$	$O(1/Y) + O(1/X)$
2D finalized	X,Y,-	Y,-,X	X,Y	Y,X	X,-,Y	X,-,Y,-	X,-,Y	$O(1/(XY)) + O(1/(XY))$	$O(1/Y) + O(1/X)$	

**Table 1.** Dense Transformer sharding annotations. X and Y are the two mesh dimensions.

Parameter count	64B		128B	256B	512B	1T
Layer count	32		64	128	256	128
M dim	8192					16384
H dim	65536					131072
Total devices	128	512	2048	2048		
Device mesh	(8,16)	(16,32)	(32,64)	(32,64)		
Batch size	64	256	1024	512	256	128
Peak memory	15.3GB	13.3GB	15.56GB	14.0GB	12.9GB	13.6GB
Step time	5.74s	6.25s	6.30s	6.31s	6.71s	7.64s
FLOPS util	62.7%	57.1%	56.9%	56.5%	54.1%	47.5%

**Table 2.** Benchmarks for dense Transformer with wide layers. The last column has 4x wider layers compared to others.

Total devices	64	128	256	64	128	256
Device mesh	(4,16)	(8,16)	(8,32)	(16,4)	(16,8)	(32,8)
Batch size	48	96	192	48	96	192
Peak memory	12.4GB	14.6GB	14.8GB	13.8GB	12.7GB	14.1GB
Step time	3.56s	3.43s	5.71s	3.10s	3.37s	3.36s
FLOPS util	39.4%	40.5%	27.1%	45.7%	41.7%	41.3%

**Table 3.** Benchmarks for 2D-sharded narrower dense Transformer. The model has 64 Transformer layers and 16 billion parameters.

the model depth increases by 2x, the maximum input batch size is roughly halved, while the step time increases only 7% from 64B to 256B. When the model size reaches 512B, the batch size becomes small and the step time increases by 13% over 256B. The last column shows a configuration with 1 trillion parameters, which is shallower than the 512B configuration, but each layer is 4x wider; as expected, the shallower 1T model can fit the same batch size as the 512B deeper model, while achieving higher efficiency due to wider layers. GSPMD achieves high overall FLOPS utilization (from 54% to 62% for most cases and 47.5% for the 512B configuration) of the TPU devices.

**Narrower dense Transformer.** Due to the relatively large batch size, activation communication is typically much more significant than weight/gradient communication. In Transformer layers, the amount of compute is  $O(MH + MND)$ , while the amount of activation communication is  $O(M)$ ; therefore, with a fixed 2D device mesh, narrower models with smaller dimensions cannot utilize the TPU’s compute power as well as wider models due to higher percentage of communication time. One mitigation is to reduce the Y dimension

Device mesh	(2,16,8)	(4,16,4)	(4,16,4)	(8,16,2)	(8,8,4)
Pipeline stages	2	4	4	8	8
Batch size	$16 \times 64$	$16 \times 64$	$32 \times 32$	$32 \times 32$	$32 \times 32$
Peak memory	14.9GB	13.3GB	13.1GB	15.0GB	11.5GB
Step time	24.0s	22.3s	22.2s	23.4s	23.7s
Raw FLOPS util	46.2%	58.0%	51.8%	54.8%	55.5%
Bubbles	5.6%	14.8%	8.0%	16.5%	16.1%
Recompute	22.3%	21.3%	21.7%	22.2%	20.6%

**Table 4.** Benchmarks for pipelining on the same model in Table 3. The device mesh has shape (L, X, Y), where L is used to shard pipeline stages, X is used for data parallelism, and Y is used for in-layer model parallelism. Raw FLOPS util is the reading from the profiler which counts padded compute (bubbles) as valid compute. The batch size is described as number of microbatches  $\times$  microbatch size.

size of the mesh, while increasing the X dimension size accordingly.

We measure the performance of a 8x narrower model which is still too big to fit on a single device: M is 4096, H is 16384, N is 64, and D is 128. It has 64 layers and 16 billion parameters in total. The results are shown in Table 3, which are consistent with our analysis above. While memory scaling is still roughly linear to the number of devices, having a smaller Y mesh dimension helps to achieve higher efficiency (with the same number of devices). With the same Y mesh dimension size, increasing the size of the X dimension allows to increase the batch size linearly with relatively constant step time.

## 5.2 Pipelined dense Transformer

This section studies the performance of GSPMD pipelining described in Section 3.3. We choose the same narrower model in Table 3, because activation communication is expensive in 2D-sharded narrower models if the Y mesh dimension is large, and having another level of parallelism could be helpful.

We use a 3D device mesh (L, X, Y) where the leading L is used to shard pipeline stages. X and Y are used in a similar way to 2D sharding (Table 1), except that weights are not sharded along X; this is because pipelining requires the input to be divided into microbatches and weight sharding on X would incur expensive per-microbatch AllGather. Nonetheless, per-device weights are sufficiently small due to L sharding.

We follow GPipe’s approach [15], where a key difference from non-pipelined configurations is that we recompute forward pass intermediate results during the backward pass, a technique known as rematerialization [10] to lower peak

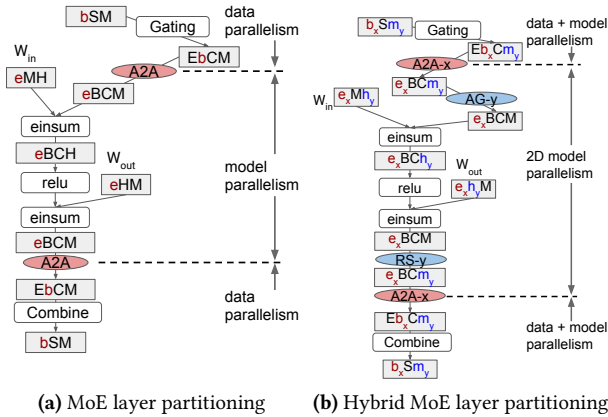


**Figure 7.** Partitioned graphs for MoE feed-forward layer and hybrid sparse and dense MoE layer. Lower-case letters indicate sharded dimensions, where different colors and subscripts denote different mesh dimensions. Collective operators: A2A is AllToAll, AG is AllGather, and RS is ReduceScatter.

memory usage. Rematerialization enables us to use larger number of microbatches to reduce pipeline bubbles.

Table 4 summarizes the performance results for configurations with 2, 4 and 8 stages. There are two major observations. 1) It is beneficial to balance the number of pipeline stages (L) and the number of in-layer model-parallel shards (Y), and the fastest configuration has 4 stages and 4 model-parallel shards. 2) Although these configurations have higher raw FLOPS utilization as reported by the profiler, the best one is still 24% slower than 2D sharding with (X=32, Y=8) (Table 3), because bubbles (compute on padded data) and recompute are overheads but counted as useful compute by the profiler.

We believe there is still value in this pipelining approach. First, other hardware platforms might not have fast, homogeneous device-to-device links in a large topology, e.g., GPU machines usually have high-speed device links only within the same server host; in-layer parallelism could be too expensive to cross hosts, while pipelining requires much smaller amounts of transfers. Second, orthogonal techniques [25] can reduce bubbles for smaller batch sizes, which can still be implemented as a python loop shardable by GSPMD; such techniques can avoid the need of recompute, making this approach competitive even for TPUs.

### 5.3 Sparse Transformer language model

Mixture-of-experts (MoE) is a recently explored research direction in scaling up the Transformer model [21, 33], where the feed-forward layer provides a collection of independent model weights (called “experts”), and each input token is operated on by only a couple of experts. Such models usually consist of both MoE and non-MoE layers in an alternating way.

Parameter count	10B	37B	145B	577B
Experts per layer	32	128	512	2048
Device mesh	(32)	(128)	(512)	(2048)
Batch size	128	512	2048	8192
Peak memory	10.8GB	11.2GB	11.2GB	11.6GB
Step time	0.98s	1.01s	1.10s	1.51s
FLOPS util	58.2%	49.8%	49.8%	46.80%
AllToAll time	2%	6%	9%	11%

**Table 5.** Benchmarks for sparse MoE Transformer with fix-sized experts.

The per-expert matrix multiplies in the MoE feed-forward layer can be expressed as Einsum operators with an extra parallel dimension, E (for experts), e.g.,  $EBCM, EMH \rightarrow EBCH$  and  $EBCH, EHM \rightarrow EBCM$ , where C is the per-expert *capacity*, i.e., the number of tokens to process per batch. Before each MoE layer, a *gating* layer computes which experts each token goes to, transforming a (B, S, M) tensor to (E, B, C, M).

To scale up the model, we can simply increase the number of experts E, as well as the input batch size so that each expert still has a reasonable amount of data to process. We found a simple yet efficient way to partition such a model:

- Use a device mesh with a single logical dimension.
- Partition the non-MoE layers by the batch dimension B. This is pure data parallelism. These layers have small weight tensors which do not need to be sharded.
- Partition the MoE layers by the expert dimension in all weights and activations. This is model-parallelism, where the large weights like  $EMH$  are fully distributed across devices.
- Switch between data and model parallelism before and after each MoE layer.

For this type of sharding, GSPMD will insert AllToAll operators to switch the sharded dimension between E and B. In the backward pass, GSPMD inserts gradient AllReduce only for non-MoE layers because there is no data parallelism for MoE layers. Figure 7a shows the partitioned forward pass.

**Performance experiments.** Except for the gating logic, the per-sample compute of this model is constant regardless of the number of experts. We study GSPMD’s scalability on this model by fixing the size of each expert, while scaling the number of experts and the batch size. Table 5 shows the performance and memory results when we set the per-device expert count to 1 (could be any constant). The step time increases only from 0.98s to 1.10s from 32 to 512 experts, as expected; when the model further increases to 2048 experts, step time increases to 1.51s. The AllToAll communication time is roughly  $O(\sqrt{\text{num\_devices}})$  on the 2D TPU device mesh, which contributes to the overhead with 2048 devices, but the main difference is that the gating compute becomes more significant with 2048 experts.

Parameter count	33B	57B	420B	804B
Experts per layer	8	16	32	64
H dim	32768		131072	
N dim	128		512	
Device mesh	(8,4)	(16,8)	(32,16)	(64,32)
Batch size	32	128	128	512
Peak memory	12.3GB	12.9GB	11.9GB	8.5GB
Step time	2.12s	2.19s	2.08s	1.92s
FLOPS util	55.3%	50.2%	50.8%	53.8%

**Table 6.** Benchmarks for hybrid sparse and dense MoE Transformer.

#### 5.4 Hybrid sparse and dense Transformer

We consider a configuration of Transformer that combines the characteristics of sparse and dense models. There are still MoE layers, but each expert is sufficiently large such that we still need to shard each expert to fit the model weights. The non-MoE layers have the same size as a single expert in an MoE layer. We use a 2D device mesh of shape  $(X, Y)$ , and the non-MoE layers are sharded the same way as the dense Transformer (Table 1). The MoE layers’ H and N dimensions are sharded on Y, while the E dimension is sharded on X. The partitioned forward pass graph is shown in Figure 7b.

**Performance experiments.** We scale the number of experts proportionally to X, and scale (batch size  $\times$  per-expert weight size) proportionally to the total number of devices. Table 6 shows the performance results of different configurations of the model using GSPMD. These configurations have roughly the same theoretical per-device compute and memory usage. As expected, the measured step time and peak memory stay relatively constant as we scale the model; the variance is much smaller than pure sparse MoE configurations (Table 5) because the hybrid configuration has fewer experts and much smaller AllToAll and gating overhead compared to the per-expert compute.

#### 5.5 Image spatial partitioning

High-resolution images are often required in object detection and segmentation tasks, but they may not fit in the memory of a single device. This section discusses *spatial partitioning* of convolution neural networks (CNNs). The goal is to shard activation tensors (along non-batch dimension) instead of model weights. As usual, GSPMD can express it with the same sharding API. In fact, sharding annotations are *required only for the model inputs*; GSPMD can propagate the shardings on the spatial dimensions to all of the convolutional layers, because they share the same set of spatial dimensions.

**Performance experiments.** We experimented with the 3D U-Net model [12], a popular dense 3D segmentation model which has been widely used in the medical image domain. With GSPMD, this model could run with the original resolution for CT images, which can be as large as 256x256x256. Spatial partitioning avoids downsampling which could affect

Device mesh	(1,1)	(1,2)	(1,4)	(1,8)	(1,16)	(4,16)	(2,32)
Image size	128x128x128					256x256x256	
Batch size	4					8	
Peak memory	14.3GB	14.8GB	7.9GB	4.5GB	2.7GB	14.9GB	8.52GB
Step time	2.99s	1.56s	0.79s	0.39s	0.19s	1.66s	0.76s
FLOPS util	47.9%	43.7%	43.5%	43.5%	43.8%	20.5%	41.2%

**Table 7.** Benchmarks for 3D U-Net with spatial partitioning. The first mesh dimension is used for data parallelism (batch partitioning), and the second mesh dimension is used for spatial partitioning. Peak memory usage includes significant device-specific padding and does not scale linearly.

accuracy. GSPMD makes this possible by simply annotating an input spatial dimension. We measure the performance of spatially partitioned 3D U-Net to evaluate GSPMD’s convolution partitioning with halo exchange (Figure 4a).

Table 7 shows two sets of measurements. We first measure GSPMD’s performance scaling with spatial partitioning only. For image size 128x128x128, GSPMD achieves nearly linear scaling with a 15.7x step time reduction on 16 partitions.

We then measure the step time when combining spatial partitioning with data parallelism to keep the same number of total devices. This time we choose image size 256x256x256, which does not fit in a single device even with per-device batch size 1. We compare the results of 16-way and 32-way spatial partitioning, and found 32-way partitioning achieves 2x higher FLOPS utilization because it enables a higher per-device batch size.

## 6 Related Work

Because programming in a distributed heterogeneous environment is challenging, particularly for high-level practitioners, deep-learning frameworks do not force users to specify precisely how the distributed computation is done. For example, TensorFlow [5] has support for data parallelism, and basic model parallelism with graph partitioning by per-node device assignment. Mesh TensorFlow [32] helps the user to build large models with SPMD-style per-operator partitioning, by rewriting the computation in a Python library on top of TensorFlow; in comparison, GSPMD partitions the graph in the compiler based on lightweight annotations, without requiring the user to rewrite the model.

GSPMD is generalized from the back-end system in our earlier work GShard [20]. GSPMD expands the sharding representation with partial tiling, and implements new techniques like recursive partitioning, making it more suitable for combined parallelism patterns.

Pipelining algorithms [13, 15, 22, 24, 36] focus on one type of parallelism, while GSPMD can be used either to express similar ideas with the help of vectorization (Section 3.3), or to work in combination of these implementations by additionally partitioning each pipeline stage. Some of these works also

provide orthogonal pipeline scheduling techniques that could be used in GSPMD to reduce pipeline bubbles.

Zero [28] presents a set of optimizations to reduce memory redundancy in parallel training devices, by partitioning weights, activations, and optimizer state separately. GSPMD is more general: it does not distinguish these tensors and dimensions, and those specific partitioning techniques can be supported by annotating the corresponding tensor dimensions with a uniform API. Weight-update sharding [38] is another automatic parallelization transformation that achieves optimizer state sharding similar to Zero, and conceptually it can be viewed as a special case for GSPMD.

Combination of in-layer model parallelism and pipelining has also been studied in previous works [4, 25]. GSPMD provides a general implementation of many of their partitioning techniques under the same sharding annotation API. For example, the scatter/gather optimization across pipeline stages in [25] is automatically enabled for all of the configurations in Table 4, because the activations are fully sharded (scatter phase) and then combined on-demand (gather phase) in the next stage (bSm and bSM tensors in Figure 6).

FlexFlow [17] uses automated search to discover the partitioning strategy of operators in a graph for better performance. While FlexFlow focuses on determining the partitioning policy, GSPMD focuses on the mechanisms to transform an annotated graph. The two are complementary to each other: GSPMD can be used to define a search space and perform the transformation, and automated search combined with GSPMD could provide a fully automated system.

Palkar et al. proposed an annotation-based parallelization framework in [26] to speed up data-intensive compute libraries like Intel MKL and Pandas. It focuses on speeding up libraries on a single multicore machine, while GSPMD instead focuses on parallelization of XLA operators on multiple connected devices.

DistIR [31] is an MPMD-style intermediate representation for distributed ML computations. It focuses on the representation itself but does not provide a transformation to automatically parallelize programs like GSPMD.

## 7 Conclusion

We presented GSPMD, a largely automated parallelization system for machine learning computation graphs. It offers a simple yet powerful API which is general enough to combine different typical parallelism patterns. GSPMD offers an intuitive auto-completion feature that enables the user to annotate only a few tensors yet the entire model is still partitioned in an efficient way. We have demonstrated that GSPMD is able to partition several image and language models on up to thousands of Cloud TPUv3 devices, with good and predictable performance and memory scaling.

## 8 Acknowledgement

We would like to thank our colleagues at XLA, Lingvo, Translate, TPU performance, and DeepMind teams for their discussions and contributions to this project. In particular, Tamas Berghammer, Marco Cornero, Cong Liu, Peter Hawkins, Mark Heffernan, David Majnemer, James Molloy, Dimitris Vardoulakis, Tong Shen, Hongjun Choi, Naveen Arivazhagan, Ankur Bapna, Orhan Firat, Macduff Hughes, and Sneha Kudugunta. We are also grateful to Mike Burrows, David Majnemer, and Naveen Kumar for their valuable and constructive feedback on earlier drafts of the paper.

## References

- [1] XLA operation semantics. [https://www.tensorflow.org/xla/operation\\_semantics](https://www.tensorflow.org/xla/operation_semantics). Online; accessed 17 April 2021.
- [2] XLA: Optimizing Compiler for TensorFlow. <https://www.tensorflow.org/xla>. Online; accessed 17 April 2021.
- [3] ONNX: Open Neural Network Exchange. <https://github.com/onnx/onnx>, 2019. Online; accessed 17 April 2021.
- [4] DeepSpeed: Extreme-scale model training for everyone. <https://www.microsoft.com/en-us/research/blog/deepspeed-extreme-scale-model-training-for-everyone/>, 2020. Online; accessed 17 April 2021.
- [5] ABADI, M., BARHAM, P., CHEN, J., CHEN, Z., DAVIS, A., DEAN, J., DEVIN, M., GHEMAWAT, S., IRVING, G., ISARD, M., KUDLUR, M., LEVENBERG, J., MONGA, R., MOORE, S., MURRAY, D. G., STEINER, B., TUCKER, P., VASUDEVAN, V., WARDEN, P., WICKE, M., YU, Y., AND ZHENG, X. TensorFlow: A System for Large-Scale Machine Learning. In *12th USENIX Symposium on Operating Systems Design and Implementation (OSDI)* (Savannah, GA, Nov. 2016).
- [6] BEZANSON, J., EDELMAN, A., KARPINSKI, S., AND SHAH, V. B. Julia: A fresh approach to numerical computing. *SIAM review* 59, 1 (2017), 65–98.
- [7] BRADBURY, J., FROSTIG, R., HAWKINS, P., JOHNSON, M. J., LEARY, C., MACLAURIN, D., AND WANDERMAN-MILNE, S. JAX: composable transformations of Python+NumPy programs.
- [8] BROWN, T. B., MANN, B., RYDER, N., SUBBLAH, M., KAPLAN, J., DHARIWAL, P., NEELAKANTAN, A., SHYAM, P., SASTRY, G., ASKELL, A., ET AL. Language models are few-shot learners. *arXiv preprint arXiv:2005.14165* (2020).
- [9] CHEN, T., MOREAU, T., JIANG, Z., ZHENG, L., YAN, E., COWAN, M., SHEN, H., WANG, L., HU, Y., CEZE, L., GUESTRIN, C., AND KRISHNAMURTHY, A. TVM: An automated end-to-end optimizing compiler for deep learning. In *Proceedings of the 13th USENIX Conference on Operating Systems Design and Implementation (USA, 2018), OSDI’18*, USENIX Association, p. 579–594.
- [10] CHEN, T., XU, B., ZHANG, C., AND GUESTRIN, C. Training deep nets with sublinear memory cost, 2016.
- [11] CHENG, Y., LEE, H., AND BERGHAMMER, T. Train ML models on large images and 3D volumes with spatial partitioning on Cloud TPUs. <https://cloud.google.com/blog/products/ai-machine-learning/train-ml-models-on-large-images-and-3d-volumes-with-spatial-partitioning-on-cloud-tpus>, 2019. Online; accessed 17 April 2021.
- [12] ÇIÇEK, Ö., ABDULKADIR, A., LIENKAMP, S. S., BROX, T., AND RONNEBERGER, O. 3D U-Net: Learning dense volumetric segmentation from sparse annotation. In *Medical Image Computing and Computer-Assisted Intervention – MICCAI 2016* (Cham, 2016), S. Ourselin, L. Joskowicz, M. R. Sabuncu, G. Unal, and W. Wells, Eds., Springer International Publishing, pp. 424–432.
- [13] FAN, S., RONG, Y., MENG, C., CAO, Z., WANG, S., ZHENG, Z., WU, C., LONG, G., YANG, J., XIA, L., DIAO, L., LIU, X., AND LIN, W. DAPPLE: A pipelined data parallel approach for training large models. In *Proceedings of the*

26th ACM SIGPLAN Symposium on Principles and Practice of Parallel Programming (New York, NY, USA, 2021), PPOPP '21, Association for Computing Machinery, p. 431–445.

- [14] GOOGLE CLOUD. Cloud TPU. <https://cloud.google.com/tpu/>. Online; accessed 17 April 2021.
- [15] HUANG, Y., CHENG, Y., CHEN, D., LEE, H., NGIAM, J., LE, Q. V., AND CHEN, Z. Gpipe: Efficient training of giant neural networks using pipeline parallelism. *CoRR abs/1811.06965* (2018).
- [16] JIA, Z., ZAHARIA, M., AND AIKEN, A. Beyond Data and Model Parallelism for Deep Neural Networks. In *Proceedings of the Conference on Systems and Machine Learning (SysML)* (Palo Alto, CA, 2019).
- [17] JIA, Z., ZAHARIA, M., AND AIKEN, A. Beyond Data and Model Parallelism for Deep Neural Networks. In *Proceedings of the Conference on Systems and Machine Learning (SysML)* (Palo Alto, CA, 2019).
- [18] KINGMA, D. P., AND BA, J. L. Adam: a Method for Stochastic Optimization. In *International Conference on Learning Representations (ICLR)* (San Diego, CA, May 2015).
- [19] KRIZHEVSKY, A., SUTSKEVER, I., AND HINTON, G. E. ImageNet classification with deep convolutional neural networks. In *Advances in neural information processing systems* (2012), pp. 1097–1105.
- [20] LEPIKHIN, D., LEE, H., XU, Y., CHEN, D., FIRAT, O., HUANG, Y., KRİKUN, M., SHAZEER, N., AND CHEN, Z. GShard: Scaling giant models with conditional computation and automatic sharding. *CoRR abs/2006.16668* (2020).
- [21] LEPIKHIN, D., LEE, H., XU, Y., CHEN, D., FIRAT, O., HUANG, Y., KRİKUN, M., SHAZEER, N., AND CHEN, Z. GShard: Scaling giant models with conditional computation and automatic sharding. In *International Conference on Learning Representations* (2021).
- [22] LI, Z., ZHUANG, S., GUO, S., ZHUO, D., ZHANG, H., SONG, D., AND STOICA, I. TeraPipe: Token-level pipeline parallelism for training large-scale language models, 2021.
- [23] MPI FORUM. MPI: A Message-Passing Interface Standard. Version 2.2, September 4th 2009. available at: <http://www.mpi-forum.org> (Dec. 2009).
- [24] NARAYANAN, D., HARLAP, A., PHANISHAYEE, A., SESHADRI, V., DEVANUR, N. R., GANGER, G. R., GIBBONS, P. B., AND ZAHARIA, M. PipeDream: Generalized pipeline parallelism for dnn training. In *Proceedings of the 27th ACM Symposium on Operating Systems Principles (SOSP)* (2019).
- [25] NARAYANAN, D., SHOYBI, M., CASPER, J., LEGRESLEY, P., PATWARY, M., KORTHIKANTI, V., VAINBRAND, D., KASHINKUNTI, P., BERNAUER, J., CATANZARO, B., PHANISHAYEE, A., AND ZAHARIA, M. Efficient large-scale language model training on gpu clusters, 2021.
- [26] PALKAR, S., AND ZAHARIA, M. Optimizing data-intensive computations in existing libraries with split annotations. In *Proceedings of the 27th ACM Symposium on Operating Systems Principles (SOSP)* (2019), pp. 291–305.
- [27] PASZKE, A., GROSS, S., MASSA, F., LERER, A., BRADBURY, J., CHANAN, G., KILLEEN, T., LIN, Z., GIMELSHEIN, N., ANTIGA, L., ET AL. PyTorch: An imperative style, high-performance deep learning library. *Advances in Neural Information Processing Systems* 32 (2019), 8026–8037.
- [28] RAJBHANDARI, S., RASLEY, J., RUWASE, O., AND HE, Y. ZeRO: Memory optimization towards training a trillion parameter models. *arXiv preprint arXiv:1910.02054* (2019).
- [29] ROESCH, J., LYUBOMIRSKY, S., WEBER, L., POLLOCK, J., KIRISAME, M., CHEN, T., AND TATLOCK, Z. Relay: a new ir for machine learning frameworks. *Proceedings of the 2nd ACM SIGPLAN International Workshop on Machine Learning and Programming Languages - MAPL 2018* (2018).
- [30] ROTEM, N., FIX, J., ABDULRASOOL, S., CATRON, G., DENG, S., DZHABAROV, R., GIBSON, N., HEGEMAN, J., LELE, M., LEVENSTEIN, R., MONTGOMERY, J., MAHER, B., NADATHUR, S., OLESEN, J., PARK, J., RAKHOV, A., SMELYANSKIY, M., AND WANG, M. Glow: Graph lowering compiler techniques for neural networks, 2018.
- [31] SANTHANAM, K., KRISHNA, S., TOMIOKA, R., FITZGIBBON, A., AND HARRIS, T. DistIR: An intermediate representation for optimizing distributed

neural networks. In *EuroMLSys '21: Proceedings of the 1st Workshop on Machine Learning and Systems* (April 2021).

- [32] SHAZEER, N., CHENG, Y., PARMAR, N., TRAN, D., VASWANI, A., KOANANTAKOOL, P., HAWKINS, P., LEE, H., HONG, M., YOUNG, C., ET AL. Mesh-tensorflow: Deep learning for supercomputers. In *Advances in Neural Information Processing Systems* (2018), pp. 10414–10423.
- [33] SHAZEER, N., MIRHOSEINI, A., MAZIARZ, K., DAVIS, A., LE, Q., HINTON, G., AND DEAN, J. Outrageously large neural networks: The sparsely-gated mixture-of-experts layer. *arXiv preprint arXiv:1701.06538* (2017).
- [34] SHAZEER, N., AND STERN, M. Adafactor: Adaptive Learning Rates with Sublinear Memory Cost. *CoRR abs/1804.04235* (2018).
- [35] SHOYBI, M., PATWARY, M., PURI, R., LEGRESLEY, P., CASPER, J., AND CATANZARO, B. Megatron-LM: Training multi-billion parameter language models using GPU model parallelism. *arXiv preprint arXiv:1909.08053* (2019).
- [36] TARNAWSKI, J., PHANISHAYEE, A., DEVANUR, N. R., MAHAJAN, D., AND PARAVECINO, F. N. Efficient algorithms for device placement of dnn graph operators, 2020.
- [37] VASWANI, A., SHAZEER, N., PARMAR, N., USZKOREIT, J., JONES, L., GOMEZ, A. N., KAISER, L., AND POLOSUKHIN, I. Attention Is All You Need. In *Proceedings of the 31st Conference on Neural Information Processing Systems (NIPS)* (Long Beach, CA, 2017).
- [38] XU, Y., LEE, H., CHEN, D., CHOI, H., HECHTMAN, B., AND WANG, S. Automatic cross-replica sharding of weight update in data-parallel training, 2020.

## A Appendix

### A.1 XLA operators for dynamism

Although XLA requires static shapes, data access can have dynamic offsets based on run-time values. Table 8 summarizes a few operators in XLA that GSPMD uses to support dynamic behaviors across different partitions.

### A.2 Halo exchange details

We first introduce the window configurations for operators like Convolution that GSPMD has to consider. Each spatial dimension in the convolution has the following set of configurations.

- **Stride** is the distance (in number of elements) that the window moves to produce the next output element.
- **Low/high padding** is the number of elements padded to the low/high end of the dimension in LHS (base).
- **Base dilation** is the dilation factor of the LHS, i.e., one plus the number of elements padded between every element (excluding low/high padding). No base dilation means the value is set to 1. Base dilation is applied before low/high padding.
- **Window dilation** is one plus the number of elements padded between every element in the RHS (window).

**Non-constant halo size.** We demonstrate that non-constant halo size is common using a simple example. Figure 8a shows a 4-way partitioned convolution, where the right halo sizes for the partitions are (1, 2, 3, 4) and can be expressed as a linear function of the partition ID:  $\text{partition\_id} + 1$ .

Figure 8b describes the sequence of operations for a general halo exchange. First, we calculate the maximum sizes of

---

**PartitionId ()**

Returns the partition id (integer) of the current device running the program.

---

**DynamicSlice (Tensor[T] operand, Tensor[int] start\_indices, List[int] size\_indices)**

Returns a slice (of shape size\_indices) from the operand tensor where the offset is given as a tensor. Used to allow each partition to select different regions of a tensor, where the dynamic offset is often calculated from PartitionId.

---

**DynamicUpdateSlice (Tensor[T] operand, Tensor[T] update, Tensor[int] start\_indices)**

Returns a tensor that replaces a sub-region of the operand tensor with the given update tensor. start\_indices specifies the offset of the region to be updated. Used similar to DynamicSlice, but to update different regions of a tensor by each partition.

---

**Iota (List[int] dimensions, int64 iota\_dimension)**

Creates an integer tensor of dimensions shape, with sequentially increasing values from 0 along the iota\_dimension (similar to std::iota(), but multi-dimensional). Used to create a mask of a partitioned tensor on each partition by comparing it against the un-partitioned dimension size.

---

**Select (Tensor[bool] pred, Tensor[T] on\_true, Tensor[T] on\_false)**

Selects each element between two tensors based on the predicate tensor. All three tensors have the same shape. Used to mask out a region of a tensor (e.g., padded region due to uneven partitions), where the mask is often computed using Iota.

---

Table 8. XLA operators used by SPMD partitioner to handle non-uniform behavior between partitions.

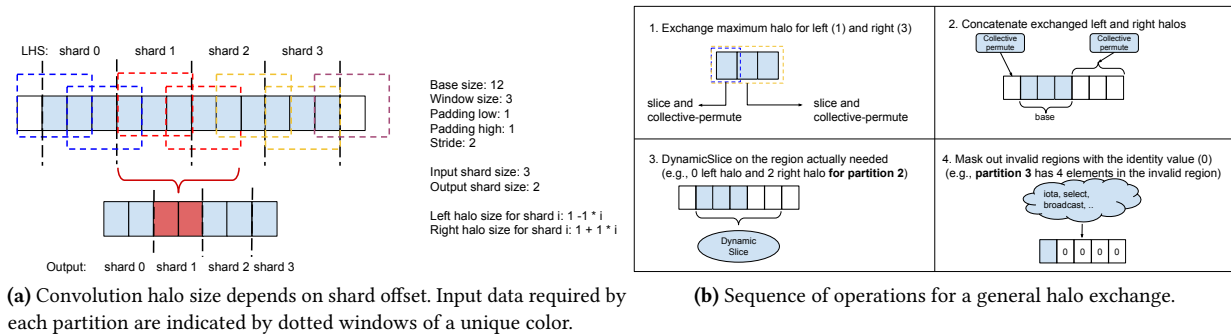


Figure 8. Non-constant halo size in a partitioned convolution and the solution with padding and slicing.

left and right halos across partitions and perform the halo exchange of the maximum size (Steps 1 and 2). Since some partitions may have excessive halos than needed, we use DynamicSlice (based on the partition ID) to get the valid region for the current partition (Step 3). Finally, some partitions may include garbage values (e.g., halos from out-of-range input data), so we apply masking as described in Section 4.1.

**Base dilation.** Base dilation adds additional complexities to halo exchange, because the offset of each partition may be positioned at the dilation holes, which makes the edges have different behavior than the interior elements. We handle base dilation in 3 cases (Figure 9).

- $stride \times per\_shard\_window\_count$  is divisible by  $dilation$ , where  $per\_shard\_window\_count$  is the number of windows to be processed by each partition (i.e., the number of output elements for each partition). This condition guarantees that

all partitions start with the same number of (interior or low) padding elements before the first data element in the LHS, so that we can use the same low padding configuration. Halo exchange occurs on the non-dilated and non-padded base region, and the limit index of required data for Partition  $i$  can be represented as  $a \times i + b$ , where  $a$  and  $b$  are both integer constants. This limit determines the right halo size.

- $stride = 1$  but  $per\_shard\_window\_count$  is not divisible by  $dilation$ . In this case, the low padding sizes vary on different partitions, but it is a static configuration. Using Pad and DynamicSlice on the operand also would not work, because those operators would be applied before dilation, so everything would be multiplied by the dilation factor. Fortunately, with  $stride = 1$ , all positions on the padded and dilated base region are valid window starts, and we can use the maximum low padding on all partitions to ensure that

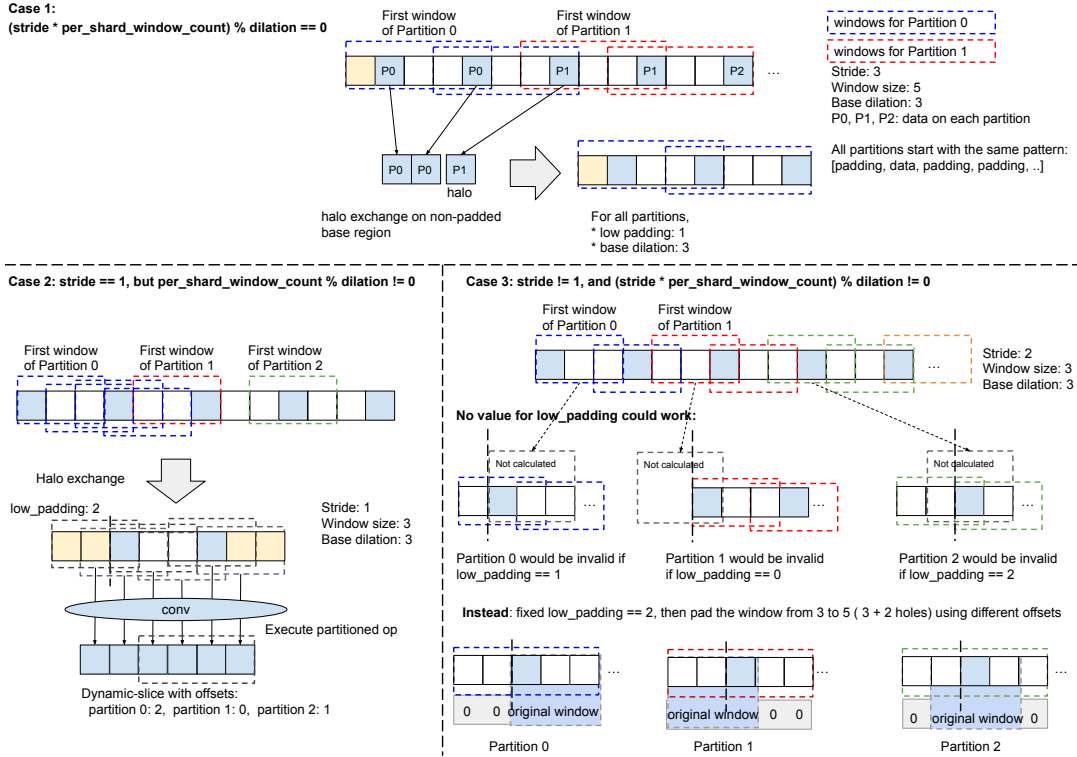


Figure 9. Convolution partitioning with base dilation.

each partition calculates all required windows, then perform a DynamicSlice on the output of the partitioned operator to remove unnecessary data. The limit index of required data on the non-padded base region for Partition  $i$  can be represented as  $(a \times i + b) / c$ , where  $a$ ,  $b$  and  $c$  are all integer constants and “/” is integer division.

- $\text{stride} \neq 1$  and  $\text{stride} \times \text{per\_shard\_window\_count}$  is not divisible by  $\text{dilation}$ . If neither of the above conditions are true, different partitions could start with different number of padding elements, and not all offsets are valid window starts. Consider the last example in Figure 9. Whatever low padding we choose, some partition will be invalid, because valid windows could be skipped since  $\text{stride} \neq 1$ . A solution to this problem is to pad the window in addition to padding the base area. We can use the maximum low padding required by the

partitions on the base area, and increase the window size by that low padding amount. The positions of the additional window padding vary on different partitions, which can be implemented as a Pad followed by a DynamicSlice. The window padding is used to mask off the unaligned elements in the base area, so that the start of the non-padding window element will be aligned with the desired start in the base area.

**Window dilation.** If the RHS is replicated, window dilation only affects the effective window size when the operator is partitioned based on its LHS. If the dilated RHS is also partitioned, which typically occurs in the gradient computation of strided convolutions, handling window dilation is still simpler than handling base dilation, because there is no low/high padding on the RHS. We skip the implementation details.